DOI 10.5162/ETTC2024/A2.3

# Link Resource SchedulingTechnology of Networked Telemetry System for LEO Constellations

Jingwei Hao[1], Jingang Zhang[1], Yan Wang[1]
[1] Beijing Institute of Astronautical Systems Engineering, Fengtai Strict, Beijing, China
hjwbit@163.com

**Abstract:**
In recent years, many mega Low Earth Orbit (LEO) satellite constellation plans to provide global Internet services have emerged internationally. The Tracking, Telemetry and Command (TT&C) system is the life line to ensure the normal operation of LEO satellites, and the telemetry systemis the key in monitoring the operation status of LEO satellites. The networked telemetry system which is based on High Earth Orbit (HEO) and Medium Earth Orbit (MEO) satellites has no coverage blind area, is applicable to various types of LEO constellations and can serve LEO satellites with abnormal attitudes. Concerning the stable-burst hybrid transmission requirements of LEO satellite telemetry data, we studies the distributed scheduling algorithm of ISL resources in the networked telemetry system. Based on the multi-agent deep reinforcement learning architecture, each MEO satellite dynamically allocates MEO beam and time slot resources according to the latest state of the system, and prioritizes the transmission of high-valuedata to increase the value of the total transmitted data of the system. Meanwhile, we designs a deep Q-network architecture to reduce network traning and storage overhead. The simulation results show that the value of the total telemetry data transmitted by the system is not less than 85% ofthe upper bound.

**Key words:** LEO constellations, Networked telemetry system, Satellite telemetry data, Resources, Deep Q-network.

## 1 Introduction

In recent years, numerous large-scale Low Earth Orbit (LEO) constellation projects providing global internet services have emerged internationally. These include the Starlink constellation, consisting of 41,926 LEO satellites[1]; the OneWeb constellation, composed of 648 LEO satellites[2]; and the Kuiper constellation, comprising 3,236 LEO satellites[3]. As of February 2023, SpaceX has successfully launched over 3,580 satellites. The OneWeb constellation, with its 648 LEO satellites, aims to provide high-speed broadband internet services to rural and remote areas. In April 2019, Amazon announced the deployment of its large broadband satellite internet constellation, Kuiper, to offer broadband internet connectivity to remote areas. This project plans to deploy 3,236 satellites within a decade, distributed across 98 orbital planes at altitudes of 590 km, 610 km, and 630 km.

In addition to these mega-LEO constellations, there are also various smaller LEO constellations currently in existence. These constellations serve purposes such as Earth observation, meteorology, disaster mitigation, and communication. As of June 2023, the global number of LEO satellites has surpassed 7,500, encompassing a wide range of functionalities. With the advancement of mega-LEO constellation projects and various functional LEO constellation plans, the number and variety of LEO satellites worldwide are expected to further increase in the future.

## 2 LEO Satellite Telemetry Systems

LEO satellite telemetry systems are primarily categorized into three types: traditional ground-based telemetry, space-based telemetry via LEO inter-satellite networks, and space-based telemetry via medium to high Earth orbit inter-satellite networks.

(a) As shown in Fig. 1, the traditional ground-based telemetry system mainly includes a mission center, a network of ground control stations, and the LEO constellation itself. When an LEO satellite is outside the line of sight of a ground control station, the telemetry data generated by the satellite can only be temporarily stored in local buffers. Once the satellite comes within the line of sight of a ground control station, it transmits both the real-time generated telemetry data and the buffered telemetry data to the ground control station via

DOI 10.5162/ETTC2024/A2.3

the satellite-to-ground link. Finally, the telemetry data is transmitted to the mission center through the ground network for further processing[4].

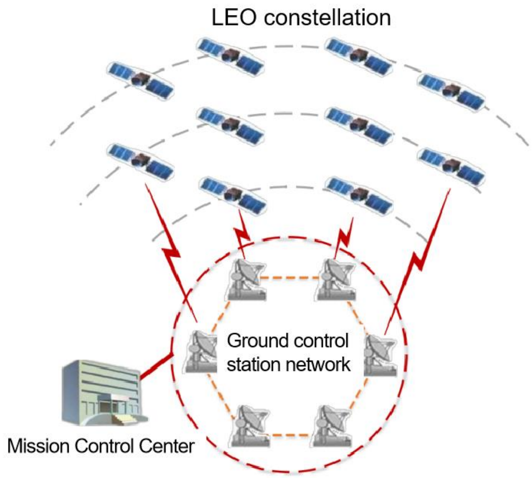


*Fig. 1.Ground-Based Telemetry System*

(b) As illustrated in Fig.2, space-based telemetry systems utilizing LEO inter-satellite networks establish inter-satellite links among the LEO satellites. When an LEO satellite is not visible to a ground control station, the telemetry data can be relayed hop-by-hop through the LEO inter-satellite network to a satellite that is within the line of sight of the ground control station. The data is then transmitted to the ground control station via the satellite-to-ground link[5].

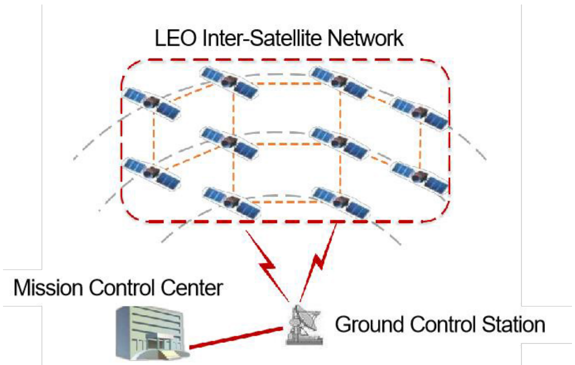


*Fig. 2.Space-Based Telemetry System Utilizing LEO Inter-Satellite Networks*

(c) As depicted in Fig.3, networked telemetry systems consist of LEO constellations and medium to high Earth orbit (MEO/HEO) constellations, with inter-satellite links existing between adjacent MEO/HEO satellites and between MEO/HEO satellites and LEO satellites. Regardless of whether the LEO satellites are visible to ground control stations, they can transmit telemetry data to the control stations and the mission center through the MEO/HEO inter-satellite network and the MEO/HEO satellite-to-ground links.

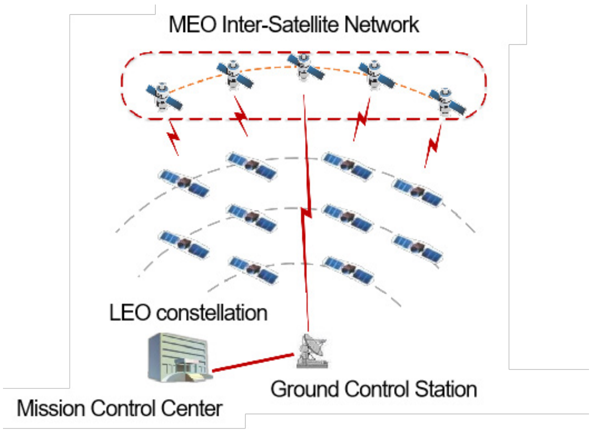


*Fig. 3.Space-Based Telemetry System Utilizing MEO/HEO Inter-Satellite Networks (Networked Telemetry)*

For ground-based telemetry systems, the return of telemetry data relies on direct line-of-sight satellite-to-ground links. Most countries find it challenging to establish control stations globally, resulting in significant telemetry coverage blind spots. Consequently, satellites outside domestic borders struggle to transmit telemetry data to the mission center in a timely manner. However, for networked telemetry systems, when LEO satellites are not visible to ground control stations, telemetry data can be transmitted continuously and without blind spots through the MEO/LEO inter-satellite network[6].

In contrast, for telemetry systems based on LEO inter-satellite networks, although multi-hop transmission through the LEO inter-satellite network can achieve continuous and blind-spot-free telemetry data transmission, this is only applicable to LEO constellations with inter-satellite links. For LEO constellations without inter-satellite links, this method is ineffective. Comparatively, networked telemetry systems do not rely on LEO inter-satellite links and are thus applicable to various types of LEO constellations. Additionally, the inter-satellite links in LEO communication constellations typically use laser or broadband microwave links. If a satellite experiences attitude anomalies, the beam of the inter-satellite link cannot be aligned, resulting in a transmission interruption. In this scenario, telemetry systems based on LEO inter-satellite networks cannot transmit telemetry data. On the other hand, networked telemetry systems use narrowband microwave links between MEO/LEO and LEO satellites, with LEO satellites using omnidirectional antennas. Therefore, even if an LEO satellite experiences attitude anomalies, it still can transmit telemetry data.

Tab.1 compares the characteristics of the three telemetry mechanisms mentioned above. From the analysis, it is evident that networked telemetry systems eliminate coverage blind spots, are applicable to various types of LEO constellations, and can service satellites with attitude anomalies. Therefore, they are more suitable for transmitting telemetry data for LEO constellations.

*Tab. 1: Comparison of Characteristics of Different Telemetry Mechanisms*

| Characteristic | Traditional Ground-Based Telemetry System | Telemetry System Based on LEO Inter-Satellite Networks | Networked Telemetry System |
|---|---|---|---|
| Telemetry Data Transmission Relies On | Yes | Yes | Yes |
| Coverage Blind Spots | Yes | No | No |
| Applicability | No | No | Yes |
| Service for Satellites with Attitude Anomalies | No | No | Yes |

## 3 Main Research and Contributions

In LEO constellations, satellite transmission power is typically limited. Additionally, to ensure telemetry data transmission even during attitude anomalies, LEO satellites are usually equipped with omnidirectional control antennas, inevitably resulting in lower transmission gains compared to directional antennas. Moreover, the distance between LEO and MEO satellites is considerable, leading to significant signal propagation attenuation in inter-satellite links between LEO and MEO satellites, thus limiting the transmission rate[7].

In a networked telemetry system, LEO satellites transmit telemetry data using omnidirectional antennas, while MEO satellites employ directional beamforming to receive telemetry data. Due to the narrow beamwidth, each MEO satellite beam can only serve one LEO satellite in a single time slot.

The term "link resources" refers to the transmission resources of different MEO satellite beams in different time slots. The orthogonal transmission resources of a single MEO satellite beam in a single time slot are defined as a single channel. Networked telemetry systems use orthogonal allocation of link resources to ensure stable and reliable telemetry data transmission.

As illustrated in Fig.4, in the MEO-LEO networked telemetry system, LEO satellites first generate telemetry data, including health status data, fault diagnosis data, program execution data, etc. This data is then transmitted via MEO-MEO links to the MEO satellites directly connected to the ground station. Finally, the MEO satellites connected to the ground station unload the telemetry data via the MEO-ground link, which is further stored and processed at the mission center. Considering that the data generation state of LEO satellites is a mixed constant-random state, this paper proposes a distributed dynamic resource scheduling architecture. In this architecture, each MEO satellite dynamically allocates MEO-LEO inter-satellite link beam and time slot resources based on the latest system state, prioritizing the transmission of high-value data to improve the overall transmission data value of the system.

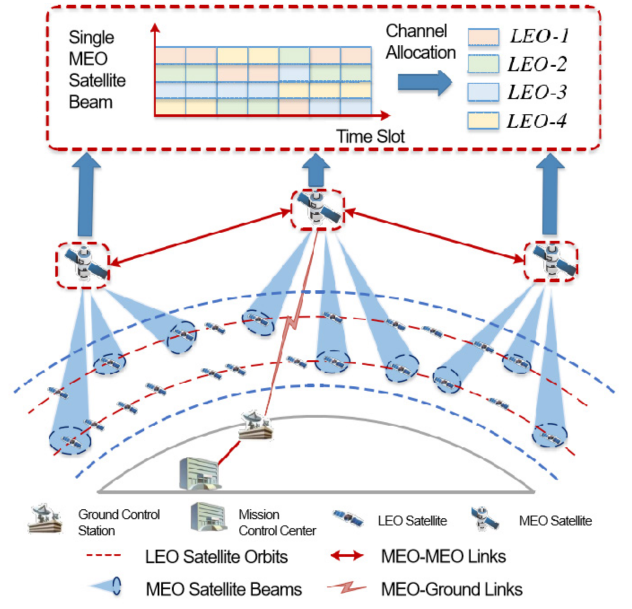


*Fig.4.Distributed Link Resource Scheduling in Networked Telemetry System*

## 4 Method

### 4.1 System Model

Considering that the data generation state of LEO satellites is a mixed constant-random state, MEO satellites utilize deep reinforcement learning to dynamically determine the channel allocation scheme. The training experience required for reinforcement learning is initially recorded locally by MEO satellites and then offloaded and stored at the mission center. Subsequently, the mission center utilizes this experience to train the Deep Q-Network (DQN) used to formulate the channel allocation scheme. Finally, the trained DQN is uploaded and deployed to the MEO satellites.

Upon completing the initial training and deployment of the DQN, the overall process of telemetry data transmission in the system is as shown in Figure 5: At the beginning of each time slot, the LEO satellite first informs the current state to the MEO satellite. Each MEO satellite possesses a wide beam to specifically collect status information from LEO satellites within its coverage area. Frequency division multiplexing is used within the wide beam to collect status information from different LEO satellites. The propagation delay between MEO and LEO is approximately 0.03s, while each time slot length is 0.25s, allowing MEO satellites to promptly obtain status information from LEO satellites. Then, based on the trained DQN, the MEO satellite determines the channel allocation scheme and broadcasts it to different LEO satellites in the current time slot. Finally, the LEO satellites transmit telemetry data to the designated MEO satellite on the allocated channels.

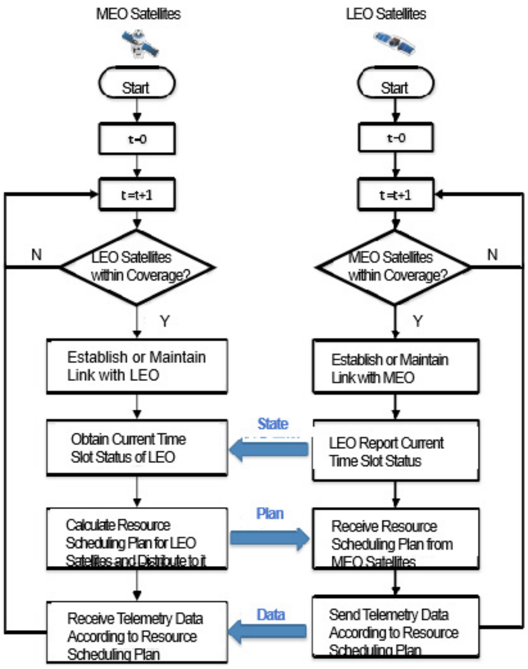


*Fig. 5. Distributed Resource Scheduling and Data Transmission Process*

This section outlines the system model and operational mechanism, detailing the utilization of deep reinforcement learning for dynamic channel allocation and the subsequent telemetry data transmission process between LEO and MEO satellites as depicted in Figure 5.

### 4.2 Problem Optimization

In the system, there are a total of $I$ LEO satellites, each equipped with one omnidirectional antenna with a transmission power of $P$. There are also $J$ MEO satellites in the system, with each satellite equipped with $K$ movable directional beams with a bandwidth of $B$. The system allocates channels for $T$ time slots, with each time slot having a length of $T_S$. In each time slot, a directional beam from an MEO satellite can only serve one LEO satellite. Here, we define the set of LEO satellites as $\mathcal{I} = \{1,2,...,I\}$, the set of MEO satellites as $\mathcal{J} = \{1,2,...,J\}$, and the set of time slots as $\tau = \{1,2,...,T\}$. The link transmission matrix is defined as $A_{I\times J\times T}$, with its matrix elements denoted as $a_{i,j}(t) = 1$. If the i-th LEO satellite transmits data to the *j*-th MEO satellite in time slot *t*, then $a_{i,j}(t) = 1$, otherwise $a_{i,j}(t) = 0$.

In order to maximize the total transmission data value of the networked telemetry system, this paper optimizes the link transmission matrix $A(t)$ and the cache transmission matrix $B(t)$. Accordingly, the objective function can be constructed as:

$$\max_{\{A(t),B(t)\}}\lim_{T\to\infty}\frac{1}{T}\sum_{t=1}^{T}V(t) \qquad (1)$$

In addition, the constraints of the networked telemetry system are as follows:

1) Each LEO satellite can be served by at most one MEO satellite in each time slot. Therefore, for $\forall i \in \mathcal{I}, t \in \mathcal{T}$, we have $\sum_{j=1}^{J} a_{i,j}(t) \leqslant 1$.

2) Since each MEO satellite has $K$ beams, at most $K$ LEO satellites can be served by the same MEO satellite in each time slot. Therefore, for $\forall j \in \mathcal{J}, t \in \mathcal{T}$, we have $\sum_{i=1}^{I} a_{i,j}(t) \leqslant K$.

3) Each LEO satellite can transmit only one type of data in each time slot. Therefore, for $\forall i \in \mathcal{I}, t \in \mathcal{T}$, we have $\sum_{l=1}^{L} b_{i,l}(t) \leqslant 1$.

Based on the analysis of the objective function and constraints mentioned above, this paper formulates the optimization problem as follows:

$$\begin{aligned} &\max_{\{A(t),B(t)|t\in\mathcal{T}\}}\lim_{T\to\infty}\frac{1}{T}\sum_{t=1}^{T}\sum_{i=1}^{I}\sum_{l=1}^{L} v_l\cdot W_{i,l}^{D}(t) \\ \text{s.t.}\quad &\sum_{j=1}^{J} a_{i,j}(t) \leqslant 1 \quad \forall i\in\mathcal{I}, t\in\mathcal{T} \\ &\sum_{i=1}^{I} a_{i,j}(t) \leqslant K \quad \forall j\in\mathcal{J}, t\in\mathcal{T} \\ &\sum_{l=1}^{L} b_{i,l}(t) \leqslant 1 \quad \forall i\in\mathcal{I}, t\in\mathcal{T} \\ &a_{i,j}(t), b_{i,l}(t)\in\{0,1\} \quad \forall i\in\mathcal{I}, j\in\mathcal{J}, l\in\mathcal{L}, t\in\mathcal{T}. \end{aligned} \qquad (2)$$

In order to maximize the total transmission data value of the system, it is essential to fully utilize the K beams of each MEO satellite. Clearly, through inference, the original problem is transformed into a problem solely related to A($t$):

$$\begin{aligned} &\max_{\{A(t)|t\in\mathcal{T}\}}\lim_{T\to\infty}\frac{1}{T}\sum_{t=1}^{T}\sum_{i=1}^{I}\max_{l\in\mathcal{L}}\left(v_l\min\left\{D_{i,l}(t),\sum_{j=1}^{J} C_{i,j}(t)\right\}\right) \\ \text{s.t.}\quad &\sum_{j=1}^{J} a_{i,j}(t) \leqslant 1 \quad \forall i\in\mathcal{I}, t\in\mathcal{T} \\ &\sum_{i=1}^{I} a_{i,j}(t) = K \quad \forall j\in\mathcal{J}, t\in\mathcal{T} \\ &a_{i,j}(t)\in\{0,1\} \quad \forall i\in\mathcal{I}, j\in\mathcal{J}, t\in\mathcal{T}. \end{aligned} \qquad (3)$$

Therefore, the original decision space size is reduced from $2^{I\times J\times T}\times 2^{I\times L\times T}$ to $2^{I\times J\times T}$.

### 4.3 Markov Decision Process

The above formula represents an optimization problem with stochastic variables, which is difficult to solve using traditional static optimization algorithms [8]. Therefore, this paper considers using reinforcement learning to dynamically allocate channels. It is worth noting that the inter-satellite and satellite-to-ground link propagation distances between LEO satellites, MEO satellites, and ground stations are far, resulting in significant propagation delays. If a centralized channel allocation architecture is adopted, the mission center will find it challenging to promptly obtain the latest status of LEO satellites and perform channel allocation. Therefore, this paper proposes letting each MEO satellite dynamically allocate channels to the LEO satellites within its coverage area. Specifically, as shown in Fig.6, each MEO satellite can be viewed as an agent, and its channel allocation can be modeled as a Markov decision process.

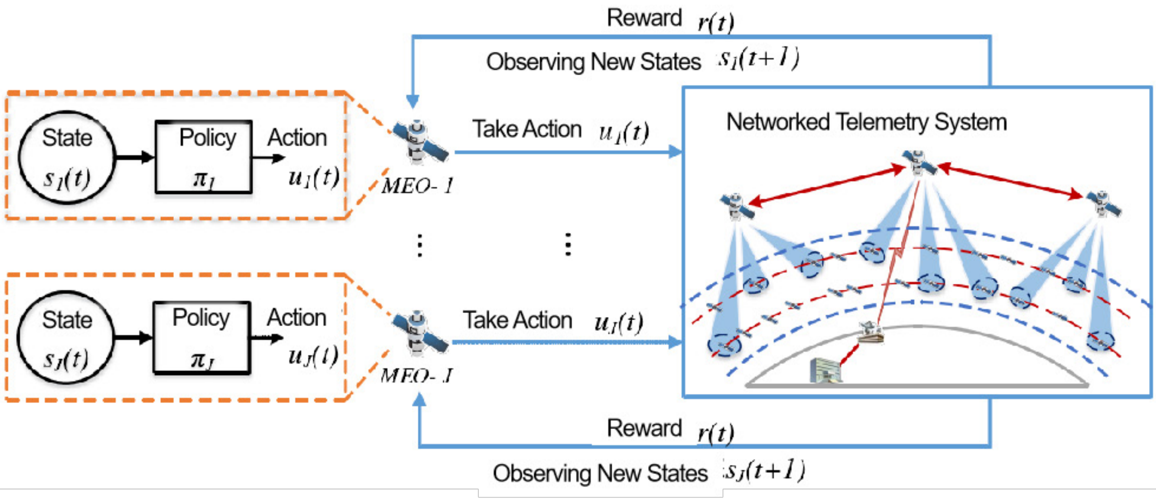


*Fig.6. Markov Decision Process Model for Distributed Scheduling Problem*

.

### 4.4 Deep Reinforcement Learning Method

For the j-th MEO satellite, after taking action $u$ in state s, it receives reward r(s,u) and transitions to state s'. For the traditional Q-learning algorithm, the Q-value is updated according to the following formula:

$$Q_j(s,u) = (1-\alpha)Q_j(s,u) + \alpha\left(r_j(s,u) + \gamma \max_{u'} Q_j(s',u')\right). \tag{4}$$

Where α ∈ (0,1] is the learning rate. The traditional Q-learning algorithm stores all action values in a Q-value table. However, when the state and action spaces are large, it is challenging to store a massive amount of action values in the Q-value table. Therefore, we adopt the method of Deep Q-learning, which uses a Deep Q-Network (DQN) with low-dimensional parameters to approximate the high-dimensional action values in the Q-value table, thus significantly reducing storage costs. The j-th MEO satellite utilizes $Q_j\left(s,u;\theta_j\right)$ computed by a DQN with parameters $\theta_j$ to approximate the actual $Q_j(s,u)$ .The optimal policy generally involves selecting the action $u$ with the highest value given state $s$[9], i.e.:

$$\pi_j^*(s,u) = \begin{cases} 1 & u = \underset{u'}{\operatorname{argmax}} Q_j(s,u') \\ 0 & \text{else} \end{cases}. \tag{5}$$

The specific training process of DQN is shown in Fig.7 After completing the network training of the $j$-th MEO satellite, the Q-function $Q_j\left(s,u;\theta_{j,train}\right)$ used to evaluate action values can be obtained. The channel allocation for the $j$-th MEO satellite will follow the optimal policy defined by Equation (5) to maximize long-term rewards.

Although DQN possesses strong fitting capabilities and can compute the values of different actions under different states, training the network can still be challenging when the action space is too large. Therefore, considering decomposing action values into combinations of sub-action values through Q-function decomposition is proposed to directly determine the connections of the network output layer, aiming to reduce network training and storage costs.

The DQN employs a fully connected structure, as depicted in Fig.8

DOI 10.5162/ETTC2024/A2.3

```
# Input: learning rate α for network training, number of training episodes N, exploration p
# Output: DQN parameters θ_(j,target) for each satellite j ∈ J

# Initialize the experience memory D_j for each satellite j ∈ J
for j = 1 to J do
    Initialize experience memory D_j as an empty set
endfor

# Randomly initialize parameters for training and target networks for each satellite j ∈ J
for j = 1 to J do
    Randomly initialize parameters for training and target networks: θ_(j,train) = θ_(j,tar
endfor

# Training loop for N episodes
for episode n = 1 to N do
    # Initialize states s_1(1), ..., s_J(1) for all satellites at time slot 1
    Initialize states s_1(1), ..., s_J(1) for all satellites

    # Loop through each time slot
    for time slot t = 1 to T do
        # Choose actions for each satellite j with ε-greedy policy
        for j = 1 to J do
            # Choose action u_j(t) with exploration probability ε or according to the optim
            if random < ε then
                Choose a random action u_j(t)
            else
                Choose action u_j(t) = argmax_u Q_j(s_j(t), u; θ_(j,train))
            endif
        endfor

        # Get rewards and next states for all satellites
        Get rewards r_1(t), ..., r_J(t) and next states s_1(t+1), ..., s_J(t+1)

        # Store experiences in memory D_j for each satellite j
        for j = 1 to J do
            Store (s_j(t), u_j(t), r_j(t), s_j(t+1)) into experience memory D_j
        endfor

        # Sample a mini-batch of experiences from D_j and update parameters θ_(j,train)
        for j = 1 to J do
            Sample a mini-batch of experiences from D_j
            Update parameters θ_(j,train)
        endfor
    endfor

    # Update target network parameters for each satellite j by copying parameters from the
    for j = 1 to J do
        Update target network parameters: θ_(j,target) ← θ_(j,train)
    endfor
endfor
```

*Fig. 7. Deep Q-Network (DQN) training*

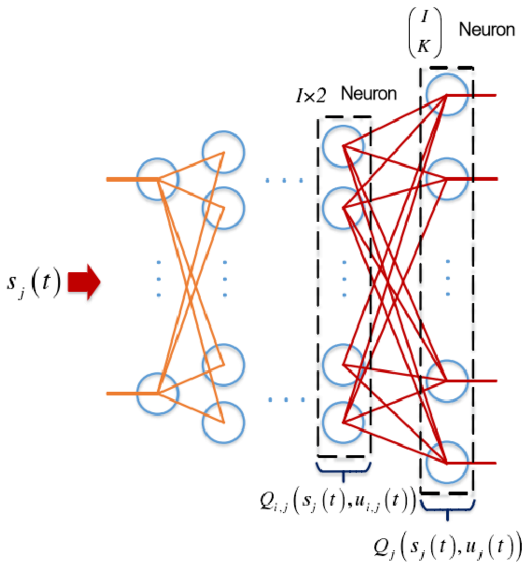


*Fig. 8. the architecture of the DQN network.*

## 5 Simulation Results

Firstly, we constructed a MEO-LEO satellite constellation for simulation, as shown in Fig. 9. The MEO constellation consists of 11 satellites evenly distributed on a circular orbit 8000 kilometers above the Earth's equator, with orbit parameters referenced from O3bmPower. The LEO constellation comprises 1584 satellites deployed in the first phase of Starlink, with orbit parameters referenced from [10]. The topological structures of the MEO and LEO constellations are illustrated in the Fig.9.

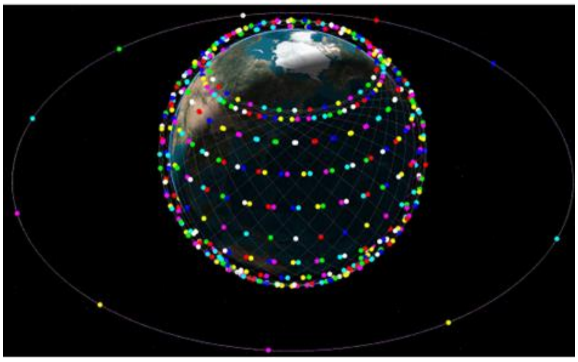

*Fig. 9. Topological Structures of the MEO and LEO Satellite Constellations*

As shown in Fig.10, after 3000 training episodes, the total transmitted data value of the system converges and tends to stabilize. Fig.11 displays the data value transmitted in different time slots after 1000, 2000, 3000, 4000, and 5000 training episodes. The transmitted data value in different time slots significantly increases as the number of training episodes increases from 1000 to 3000. Subsequently, as the number of training episodes increases from 3000 to 5000, the transmitted data value in different time slots remains relatively stable.

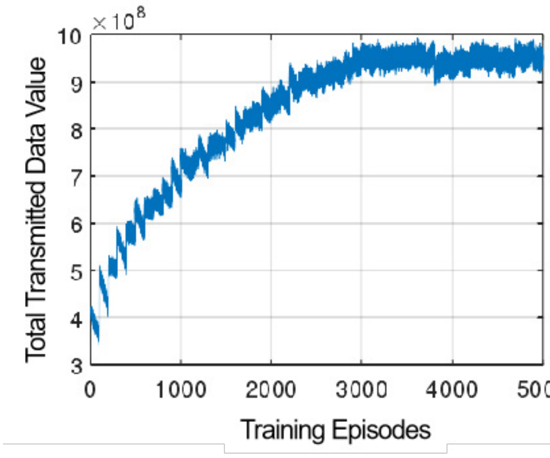


*Fig. 10. Convergence of the Distributed Scheduling Algorithm*

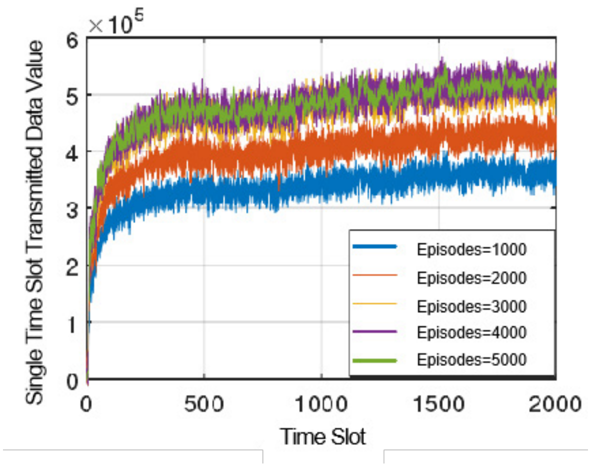


*Fig. 11. The Data Value Transmitted in Different Time Slots after Training with Varying Numbers of Episodes.*

## 6 Conclusion

This paper constructs a Markov Decision Process (MDP) based on multi-agent reinforcement learning framework for dynamic channel allocation. Considering the vast state and action space of the Markov Decision Process, a Deep Q Network (DQN) is employed to compute action values. The original action function is decomposed into a combination of Q functions for multiple sub-actions, and the output layer connections of the Deep Q Network (DON) are further designed to significantly reduce the training and storage overhead of the DQN. Finally, numerical simulations are conducted to verify the performance of the proposed channel allocation algorithm under different system parameters. Simulation results demonstrate that the proposed channel allocation algorithm achieves higher total transmitted data value compared to other benchmark algorithms, surpassing 85% of the performance upper bound.

## References

[1] Wang I, Li L, Qin Z, et al. Capacity analysis of LEO mega-constellation networks[J].IEEE Access, 2022, 10:18420-18433.

[2] Chen Q, Chen X, Yang L, et al. A distributed congestion avoidance routing algorithm in mega-constellation network with multi-gateway[I.Acta Astronautica, 2019, 162:376-387

[3] Lai Z, Li H, Li J. Starperf: Characterizing network performance for emerging mega-constellations[C]//2020 IEEE 28th International Conference on Network Protocols (ICNP). IEEE, 2020: 1-11.

[4] Garg V K, Sharma C D. Engineering and performance evaluation of TTC ground station[J]. IETE Technical Review, 1989, 6(5): 380-386.

[5] Pan X, Zhan Y, Zeng G, et al. TT&C capacity analysis of mega-constellations: How many satellites can we support?[C]//ICC 2022-IEEE International Conference on Communications. IEEE, 2022: 2393-2398.

[6] Zhan Y, Zeng G, Pan X. Networked TT&C for mega satellite constellations: A security perspective[J]. China Communications, 2022, 19(9): 58-76.

[7] Jia L, Zhang Y, Yu J, et al. Design of mega-constellations for global uniform coverage with inter-satellite links[J]. Aerospace, 2022, 9(5): 234.

[8] Sutton R S, Barto A G. Reinforcement learning: An introduction[M]. MIT press, 2018.

[9] Arulkumaran K, Deisenroth M P, Brundage M, et al. Deep reinforcement learning: A brief survey[J]. IEEE Signal Processing Magazine, 2017, 34(6): 26-38.

[10] Albulet M. Spacex v-band non-geostationary satellite system[J]. Federal Commun. Commission, Washington, DC, USA, Tech. Rep. SAT-LOA-20161115-00118, 2017.